AD-A131 694 ALBORAN SEA MODELING(U) JAYCOR ALEXANDRIA VA 1/1
R H PRELLER 25 APR 83 JAYCOR-J206-83-004/6216
N00014-81-C-0810

UNCLASSIFIED F/G 8/3 NL

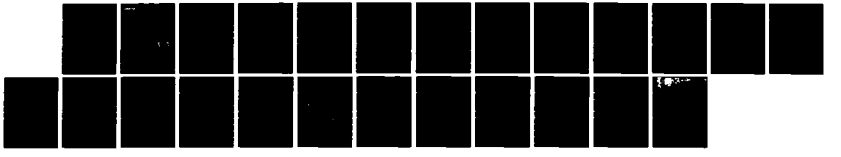

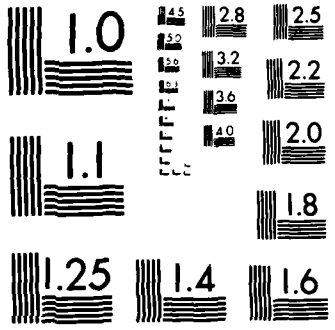

MICROCOPY RESOLUTION TEST CHART
NATIONAL BUREAU OF STANDARDS 1963-A

JAYCOR

(1)

AD A131694

ALBORAN SEA MODELING

J206-83-004/6216

Final Report

by

Ruth H. Preller

April 25, 1983

Prepared for:

Naval Ocean Research and Development Activity
NSTL Station, MS 39529

Under:

Contract Number N00014-81-C-0810

205 South Whiting Street • Alexandria, Virginia 22304 • (703) 823-1300

UNCLASSIFIED

SECURITY CLASSIFICATION OF THIS PAGE (When Data Entered)

REPORT DOCUMENTATION PAGE		READ INSTRUCTIONS BEFORE COMPLETING FORM
1. REPORT NUMBER J206-83-004/6216	2. GOVT ACCESSION NO.	3. RECIPIENT'S CATALOG NUMBER
4. TITLE (and Subtitle) ALBORAN SEA MODELING		5. TYPE OF REPORT & PERIOD COVERED Final Report - 09/02/81 thru 11/01/82
		6. PERFORMING ORG. REPORT NUMBER J206-83-004/6216
7. AUTHOR(s) Ruth H. Preller		8. CONTRACT OR GRANT NUMBER(s) N00014-81-C-0810
9. PERFORMING ORGANIZATION NAME AND ADDRESS JAYCOR 205 South Whiting Street Alexandria, VA 22304		10. PROGRAM ELEMENT, PROJECT, TASK AREA & WORK UNIT NUMBERS A002
11. CONTROLLING OFFICE NAME AND ADDRESS Naval Ocean Research and Development Activity NSTL Station, MS 39529		12. REPORT DATE April 25, 1983 13. NUMBER OF PAGES 20 pages
14. MONITORING AGENCY NAME & ADDRESS(if different from Controlling Office)		15. SECURITY CLASS. (of this report) UNCLASSIFIED 15a. DECLASSIFICATION/DOWNGRADING SCHEDULE

16. DISTRIBUTION STATEMENT (of this Report)

1 - Scientific Officer
1 - Administrative Contracting Officer
6 - NRL, Code 2627
12 - Defense Technical Information Center
1 - Office of Naval Research, Western Regional Office

APPROVED FOR PUBLIC RELEASE
DISTRIBUTION UNLIMITED

17. DISTRIBUTION STATEMENT (of the abstract entered in Block 20, if different from Report)

18. SUPPLEMENTARY NOTES

19. KEY WORDS (Continue on reverse side if necessary and identify by block number)

20. ABSTRACT (Continue on reverse side if necessary and identify by block number)

DD FORM 1 JAN 73 1473 EDITION OF 1 NOV 65 IS OBSOLETE
S/N 0102-LF-014-6601

UNCLASSIFIED

SECURITY CLASSIFICATION OF THIS PAGE (When Data Entered)

TABLE OF CONTENTS

1.		INTRODUCTION	1
2.		THE MODEL	4
3.		MODEL RESULTS	8
	3.1	THE PIVOTAL EXPERIMENT	8
	3.2	THE EFFECT OF INFLOW ANGLE	9
	3.3	PORT LOCATION	10
	3.4	BOUNDARY EFFECTS	10
	3.5	SHEAR AT INFLOW	13
	3.6	ADDITION OF LOWER LAYER FLOW	14
4.		SUMMARY AND FUTURE WORK	18
		REFERENCES	19

ALBORAN SEA MODELING

1. INTRODUCTION

The circulation of the Alboran Sea is dependent on both Atlantic and Mediterranean waters. Atlantic water flows through the narrow (20 km wide) and shallow (300 m deep) Strait of Gibraltar into the Alboran Sea forming a 150-200 m deep surface layer (Ovchinnikov, 1966; Lanoix, 1974; Katz, 1972). Mediterranean water enters the Alboran at its open eastern boundary and flows slowly westward in the form of an intermediate and lower layer. It has been suggested that even the deepest water can exit through the Strait (Stommel et al., 1973; Gascard, 1982). The large volume transport of inflowing Atlantic water, 1 to 2 X 10^6 m^3/sec, (Lacombe, 1971; Bethoux, 1979; Lacombe, 1982) retains its identity as a narrow (30 km wide) jet with initial speeds of 100 cm/sec near the Strait (Lacombe, 1961; Peluchon and Donguy, 1962; Grousson and Faroux, 1963; Lanoix, 1974; Cheney, 1977; Petit et al., 1978; and Wannamaker, 1979). The jet enters the basin and flows northeast to approximately 4°W, curves southward and then splits (Figure 1). Part of the jet flows to the west and is incorporated in an anticyclonic gyre, while the remainder flows southeast to Cape Tres Forcas and then along the African coast forming the southern periphery of a cyclonic circulation.

Satellite infrared imagery indicates variations in the shape, location and intensity of the persistent anticyclonic gyre which dominates the western Alboran Sea. Hydrographic data and satellite infrared images support the year-round persistence of the gyre, although its size and location varies (Stevenson, 1977; Cheney, 1978; Wannamaker, 1979; Burkov et al., 1979; Gallagher et al., 1981). In the eastern portion of the Alboran Sea a general pattern of alternating cyclonic and anticyclonic circulations has been observed (Cheney, 1978; Lanoix, 1974). Satellite imagery shows that, compared to the western Alboran, this circulation pattern is far more variable and of smaller scale.

A study of circulation in the Alboran Sea begins by using the simplest model capable of simulating major features of the circulation. This is a reduced gravity model in a semi-enclosed,

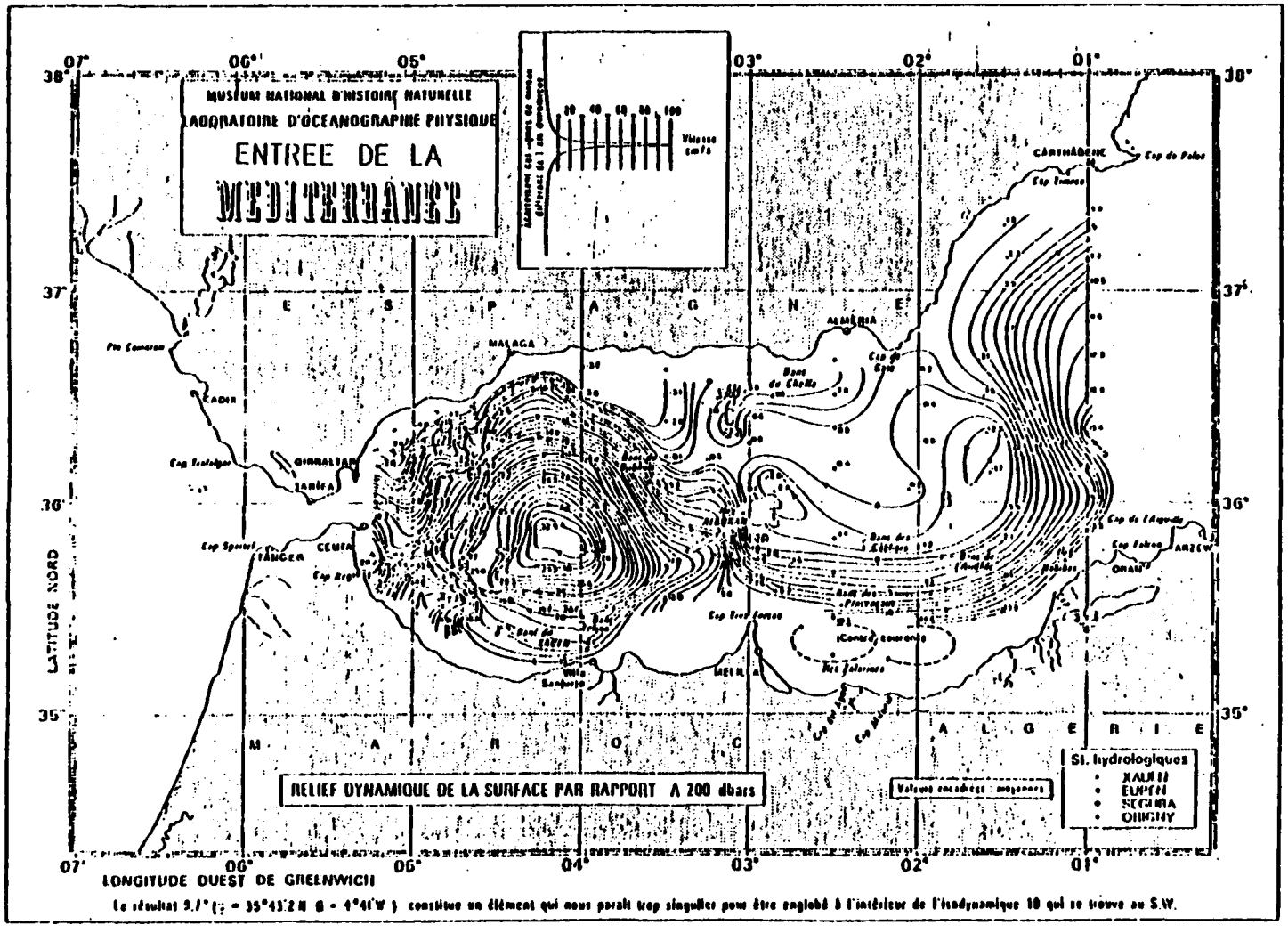

Figure 1. Dynamic topography of the surface relative to 200 dbar for July-August 1962. Overlaid rectangle is the model Alboran Sea geometry. (Lanoix, 1974)

rectangular domain. It is essentially a model of the first baroclinic mode and does not permit baroclinic instability or the inclusion of bottom topography. We then progress to the two layer model eventually including topography and the geometry of the Alboran Sea. The model formulation and parameters are discussed in Section 2. In Section 3 the model results are presented in terms of a pivotal experiment and some deviations from it. Section 3.1 discusses the pivotal experiment. The subsections which follow investigate the influences of (3.2) inflow angle, (3.3) port location, (3.4) boundary effects, (3.5) inflow vorticity and (3.6) the addition of lower layer flow.

2. THE MODEL

A nonlinear reduced gravity model, developed for the Gulf of Mexico by Hurlburt and Thompson (1980), has been adapted for the Alboran Sea. The model equations are solved numerically using an economical semi-implicit scheme. The model consists of an active upper layer and a lower layer which is infinitely deep and at rest. It is stably stratified and has a fixed density contrast between two immiscible layers. The model assumes a hydrostatic, Boussinesq fluid in a rotating right-handed coordinate system on a β-plane. The vertically integrated model equations are

$$\frac{\partial \vec{V}_1}{\partial t} + (\nabla \cdot \vec{V}_1 + \vec{V}_1 \cdot \nabla)\,\vec{v}_1 + \hat{k} \times f\vec{V}_1 = -\, g' h_1 \nabla h_1 + (\vec{\tau}_1 - \vec{\tau}_2)/\rho + A\nabla^2 \vec{V}_1$$

$$\frac{\partial h_1}{\partial t} + \nabla \cdot \vec{V}_1 = 0$$

where

$$\nabla = \frac{\partial}{\partial x}\,\hat{i} + \frac{\partial}{\partial y}\,\hat{j}$$

$$\vec{V}_1 = h_1 \vec{v}_1 = h_1\,(u_1 \hat{i} + v_1 \hat{j})$$

$$g' = g(\rho_2 - \rho_1)/\rho$$

$$f = f_o + \beta(y - y_o)$$

$$\tau_i = \tau_i^x\,\hat{i} + \tau_i^y\,\hat{j}$$

and x and y are tangent-plane Cartesian coordinates with x directed eastward and y northward, u_1 and v_1 are the eastward and northward velocity components in the upper layer, h_1 is the upper layer thickness, t is time, g is the acceleration due to gravity, ρ_i is the density of

seawater in layer i, f_0 and y_0 are the values of the Coriolis parameter and the y-coordiante at the southern boundary, $\vec{\tau}_1$ is the wind stress, and $\vec{\tau}_2$ is the interfacial stress. The remaining parameters are defined in Table 1.

Table 1
MODEL PARAMETERS FOR THE PIVOTAL EXPERIMENT

Parameter	Definition	Value
A	eddy viscosity	250 m^2 sec^{-1}
β	(df/dy)	2 x $10^{-11}m^{-1}sec^{-1}$
f_o	Coriolis parameter	8 x $10^{-5}sec^{-1}$
g'	reduced gravity due to stratification	.02 m sec^{-2}
H_1	undisturbed upper layer depth	200 m
H_2	undisturbed lower layer depth	∞
L_x X L_y	horizontal dimensions of the model domain	600 km x 160 km
Δx X Δy	horizontal grid spacing for each dependent variable	10 km x 5 km
Δt	time step	1 hour
$\vec{v}_{1in}$	inflow velocity	100 cm/sec
α	angle of inflow	21° north of east
t_s	inflow spin up time constant	30 days

Figure 1 shows the model domain superimposed on a map of the Alboran Sea. This domain is 600 km x 160 km with 10 km x 5 km grid resolution for each dependent variable. Forcing is due solely to prescribed inflow through the western port (Strait of Gibraltar). Inflow is exactly compensated by outflow through an open eastern boundary. This is accomplished by allowing normal flow at the eastern boundary to be self-determined and by imposing an integral constraint on

total mass outflow (Hurlburt and Thompson, 1980). Except at the inflow and outflow ports, the boundaries are rigid and a no-slip condition is prescribed on the tangential flow. Along the eastern boundary the tangential component is set to zero one-half grid distance outside the physical domain.

The model parameters for the pivotal experiment are given in Table 1. In this experiment the western (inflow) port is centered 102 km from the southern boundary and is 15 km wide, a width appropriate for the Strait of Gibraltar at a depth of 100 m. The specification of the model forcing is accomplished in either of two ways:

- by prescribing velocity ($\vec{v}_{1in}$) or
- by prescribing transport ($\vec{V}_{1in}$) and allowing the model to determine the inflow velocities.

The former is used in the pivotal experiment. The total inflow transport used in the model (2.5×10^6 m^3/sec) is higher than observed. This value is necessary to drive a unifrom inflow profile for $\vec{v}_1$ or $\vec{V}_1$ with speeds of ~ 100 cm/sec, given the port width and upper layer depth in Table 1. The inflow is spun up with a time constant of 30 days to minimize the excitation of high frequency waves. The angle of inflow was varied based on direct observations (Lacombe, 1961) and on inferences from satellite imagery. The standard inflow angle was chosen to be 21° north of east based on the geometric orientation of the Strait of Gibraltar. Possibly important wind forcing (Ovchinnikow et al., 1976; Mommsen, 1978) is neglected to allow focus on the circulation driven by flow through the Strait of Gibraltar.

Substantial effort was made to assure that unphysical aspects of the model such as the grid resolution and the time step did not significantly influence the model solution. The open eastern boundary condition was a special concern and one important test of its influence is discussed in Section 3.4. The integral constraint on the total mass flux through the eastern boundary resulted in plane wave reflection of sufficient amplitude to pose a significant problem. The eddy viscosity (A) chosen for the model is the minimum value which prevents any visible oscillation in the solution due to this reflection. An eddy viscosity 2½ times smaller yielded nearly the same solution except for some

unphysical oscillations. A viscous boundary layer using a linear interfacial stress was also applied near the open eastern boundary in an effort to damp the oscillations due to the integral constraint. The maximum value for the drag coefficient was 10^{-3} sec^{-1} at the eastern boundary. It decreased exponentially away from the boundary with an e-folding width of 50 km. This aided only slightly in damping the reflection from the integral constraint. Except for the viscous boundary layer, the interfacial stress was zero.

3. MODEL RESULTS

Over forty numerical experiments were performed for the Alboran Sea. Some preliminary results will be presented in terms of a pivotal experiment and selected variations from it. Most of the numerical solutions evolved to a steady state in about one year.

3.1 THE PIVOTAL EXPERIMENT

The pivotal experiment uses the parameters in Table 1. Figure 2 shows the steady state model solution (day 500) in terms of the pycnocline anomaly (PA). The PA is the divation of the interface between the upper and lower layers from its initial flat position at 200 m depth. Downward deviations are positive (upper layer thicker ti initially). The most striking features are

- a meandering current which traverses the model domain fr west to east,
- a strong anticyclonic gyre in the western 249 km of the basin, and
- a weak cyclonic circulation to the east.

This pattern is very similar to the temperature field shown in a satellite image and to Lanoix's dynamic topography (Figure 1).

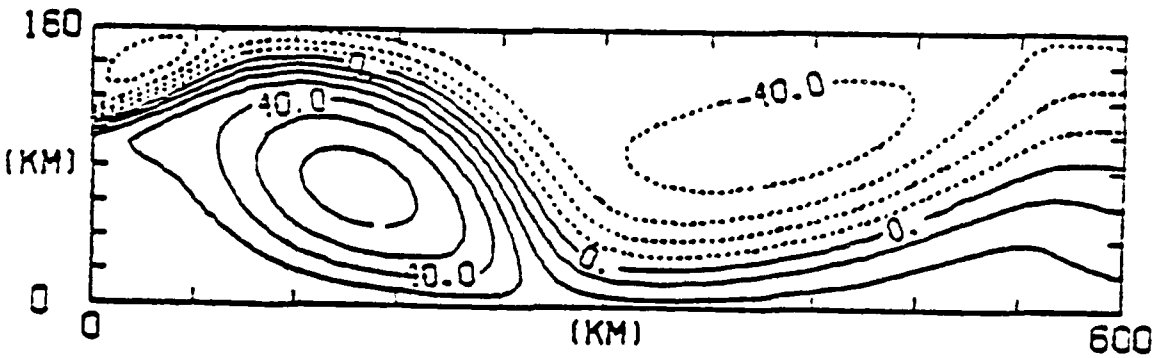

Figure 2. PA (pynocline anomaly) of the pivotal case solution at day 500. Inflow angle is 20° north of east. Solid contours are positive (downward) deviations. Dashed contours are negative (upward) deviations. Contour interval is 10 m.

In rotating tank experiment, Whitehead and Miller (1979) attempted to simulate the Alboran Gyre using a density driven current.

They suggest that the dimensions of the gyre depend on a coastline feature, Cape Tres Forcas. It has also been suggested by Porter (1976) that the dimensions of the gyre are directly related to the bottom topography with Alboran Island acting as the eastern boundary of the gyre. Yet the reduced gravity model is able to simulate an Alboran Gyre with realistic dimensions, while including neither coastline irregularities nor bottom topography. The model gyre is also a persistent rather than a transient feature of the flow, again in accord with observations noted earlier.

3.2 THE EFFECT OF INFLOW ANGLE

The circulation pattern in the pivotal experiment (Figure 2) and satellite imagery suggest that the inflow angle may exert an important influence on the meandering current and the Alboran Gyre. Thus, a number of experiments were carried out varying the inflow angle. One experiment used the standard parameters from Table 1 except that the inflow entered the model domain normal to the western boundary. In the steady state solution for this case (Figure 3), the jet enters the basin flowing due east, but quickly veers southward. The anticyclonic gyre in the western part of the basin is restricted to a much smaller north-south extent than in the standard case. The cyclonic circulation to the east is intensified and a new anticyclonic flow appears in the eastern 200 km. This circulation pattern is similar to that of the sea surface temperature seen in the satellite infrared imagery.

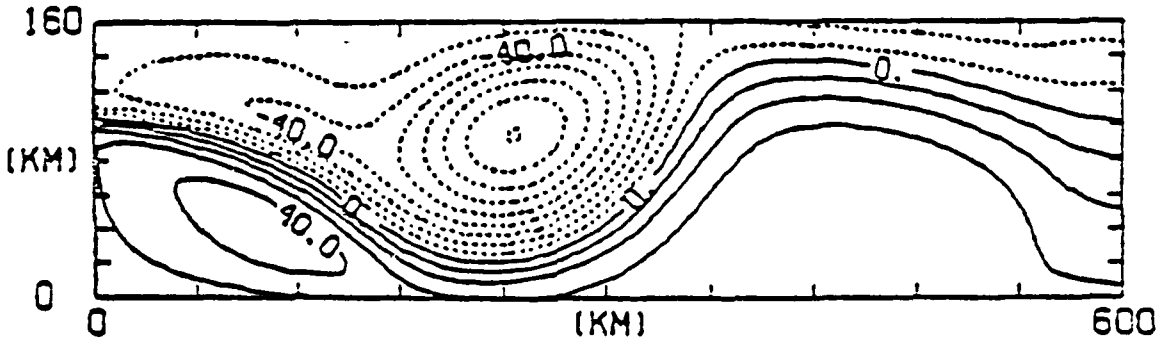

Figure 3. PA of the pivotal case at day 500 but with due east inflow. Contour interval is 10 m.

3.3 PORT LOCATION

The next set of experiments was designed to observe the importance of the north-south location of the inflow port. If the Strait of Gibraltar was located south of the basin center, how would the circulation pattern be affected? Two such experiments used the standard parameters of Table 1 except that the port was centerd 7 km south of the center of the western boudary and the inflow angles were those of Figure 2 (standard 21° north of east) and Figure 3 (0°). The steady state solutions are presented in Figure 4. Figure 4a, with the angles inflow of the standard case, shows

- an anticyclonic gyre smaller than that of the standard case in the western part of the basin,
- a strong cyclonic circulation in the central part, and
- a weak anticyclonic circulation in the eastern part.

When the inflow enters flowing due east (Figure 4b) the western gyre is even smaller than in Figure 4a and the two gyres to the east are slightly stronger. Clearly, the entrance of the Atlantic water in the northern half of the Alboran Sea facilitates the development of an Alboran Gyre of large north-south extent.

3.4 BOUNDARY EFFECTS

The influences of the domain size and the open eastern boundary were also investigated. As described in Section 2, the pivotal experiment includes a viscous boundary layer near the open eastern boundary. One test compared the pivotal experiment with this boundary layer (Figure 2) to an identical experiment without it (not shown). Except in the region of the viscous boundary layer, the results were almost identical. In the experiment without the boundary layer, the current maintained its cross-sectional sturcture as it approached and passed through the open eastern boundary. When it was included, the PA contours spread out in the viscous boundary layer and the jet structure disintegrated to a more uniform flow (see Figure 2).

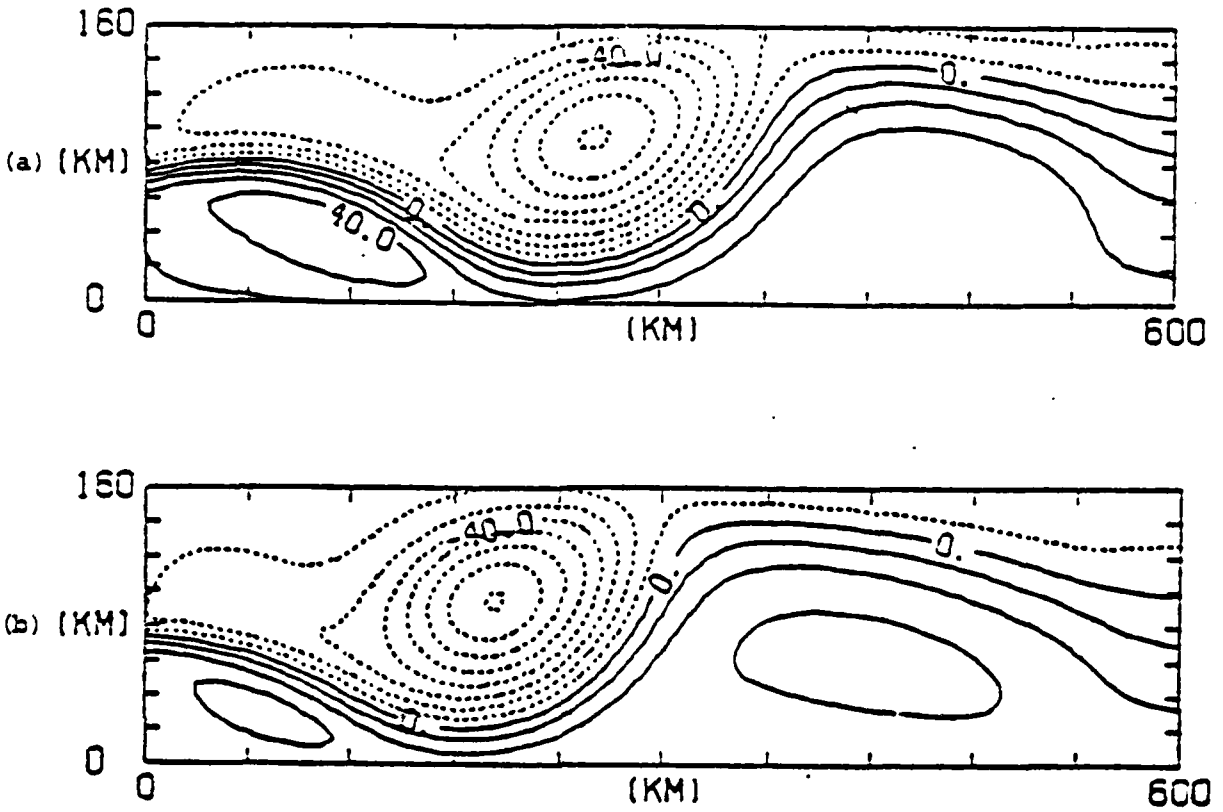

Figure 4. PA of the pivotal case at day 500 but with the port centered 7 km south of the center of the western boundary. (a) Inflow angles 21° north of east; (b) due east inflow. Contour interval is 10 m.

Numerical experiments were also performed to determine if the open eastern boundary was seriously distorting the solution. Figure 5 shows the results of a critical test. It compares two solutions which differ only in the east-west extent of the model domain. In each case there is a viscous boundary layer near the open eastern boundary. In this test, changing the location of the open eastern boundary caused only minor changes in the solution in the western 400 km of the model domain. The eastern 100 km in Figure 5b differs from the same region in Figure 5a, due mostly to the viscous boundary layer in the vicinity of the open boundary.

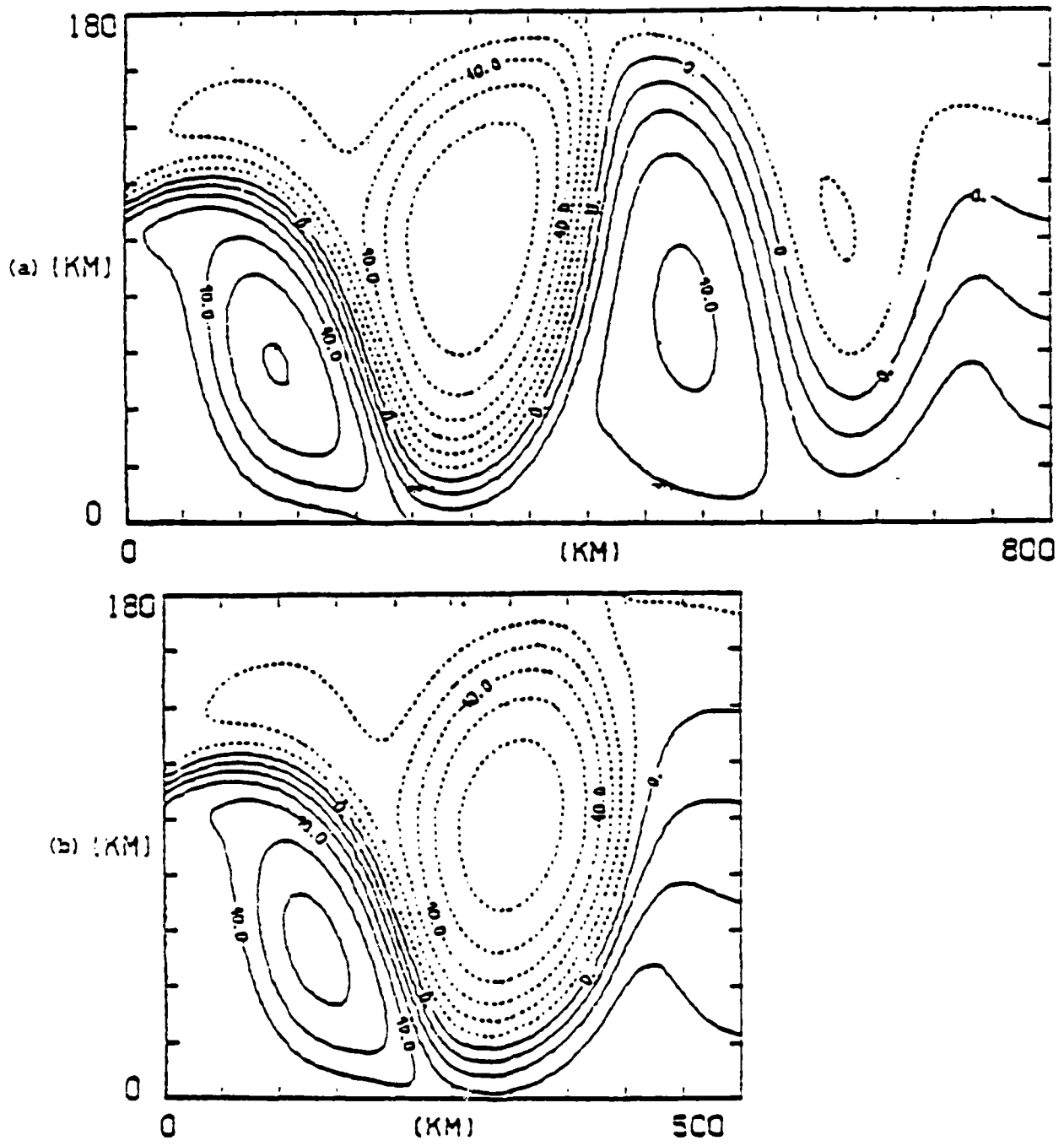

Figure 5. PA of the pivotal case at day 190 but with different dimensions, (a) 180 km x 800 km basin; (b) 180 km x 500 km basin. Scale factor for these figures x:y is 1:2.5. Contour interval is 10 m.

The effect of the north-south extent of the basin was examined by doubling the y-dimension of the standard experiment (Figure 2) and keeping the port location slightly north of the basin center. Figure 6 shows the flow entering the basin at the standard angel of 21° and then curving southward in a manner similar to Figure 4a. Even though the north-south extent of the basin has been doubled, the northern and southern boundaries of the domain still limit the north-south scale of the current meanders. Despite a large increase in the amplitude of the meanders in Figure 6, the wavelengths in Figure 4a and Figure 6 are almost the same. A striking feature in Figure 6 is the downstream amplification of the current meanders. Less dramatic examples of this appear in some of the other figures. It should be noted that this and all the other solutions are steady and not unstable.

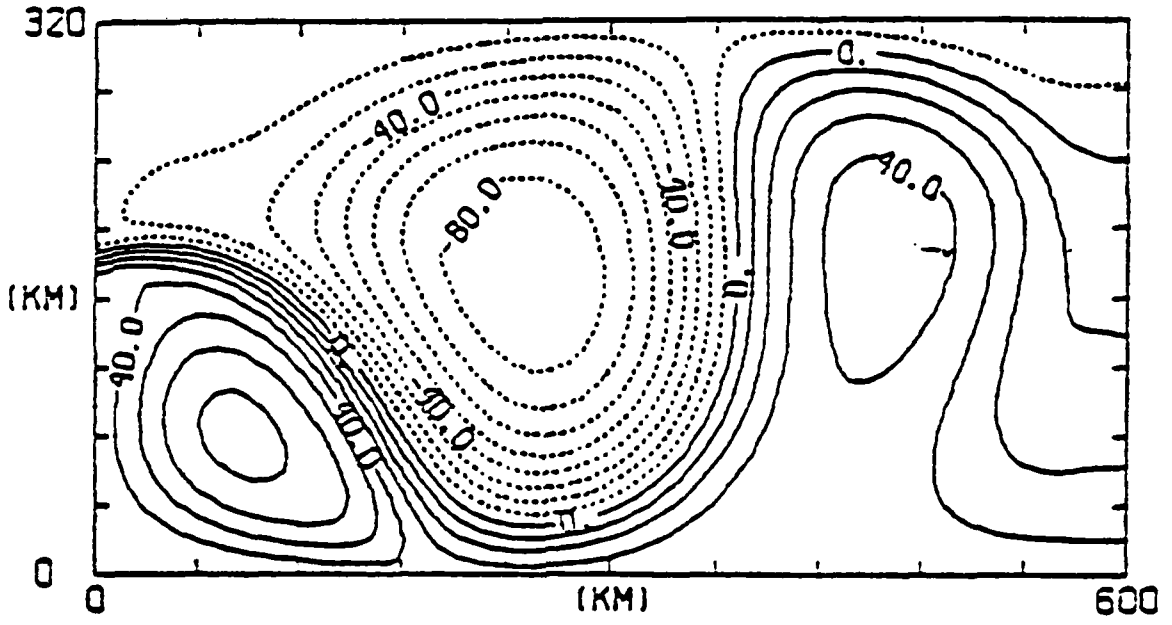

Figure 6. PA at day 600 of an experiment where the north-south dimension of the basin has been extended to 320 km, contour interval is 10 m.

3.5 SHEAR AT INFLOW

In all the experiments discussed so far, the inflow has been prescribed as a velocity profile ($\vec{v}_1$). However, in this model the inflow may also be prescribed in terms of transport ($\vec{V}_1$). In the latter

case, the model partially controls the inflow velocity profile through the geostrophic tilt in the interface. Figure 7 shows a steady state solution for an experiment similar to that shown in Figure 4b, except that $\vec{V}_1$ is prescribed instead of $\vec{v}_1$. In both cases the inflow is eastward. In Figure 7 the prescribed inflow transport is 2.5 x 10^6 m^3/sec. This yields inflow velocities similar to Figure 4b, but the geostrophic tilt in the interface introduces a shear ($\partial u/\partial y$) of 1.54 x 10^{-5} sec^{-1} at inflow. Without the shear (Figure 4b) the current turns southward after inflow, but with the shear (Figure 7) the current turns northward. In addition, Figure 7 shows a larger Alboran Gyre which is further to the east and a small cyclonic gyre in the northwest corner. The possibility that vorticity at inflow turns the incoming Atlantic water northward has been suggested by Nof (1978).

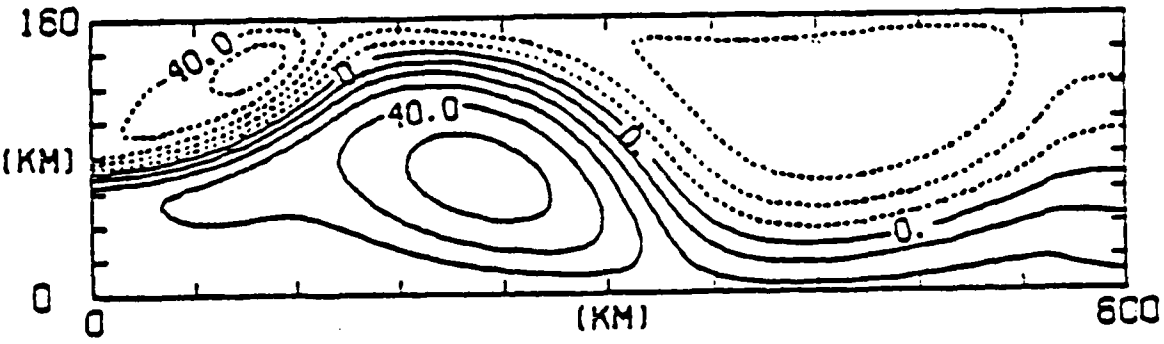

Figure 7. PA at day 500 of a case identical to the case represented in Figure 4b except that the model is forced with a prescribed transport. Contour interval is 10 m.

3.6 ADDITION OF LOWER LAYER FLOW

In the Alboran Sea region of the Mediterranean, circulation may be divided into two layers; an upper eastward moving layer, 200 m deep and a lower westward moving layer 2400 m deep. Figure 8 is a representation of the two layer model. The equations used are those presented in Section 2, where the subscript 1 is replaced by 2 and the pressure term is replaced by

$$- h_2 \nabla P_2$$

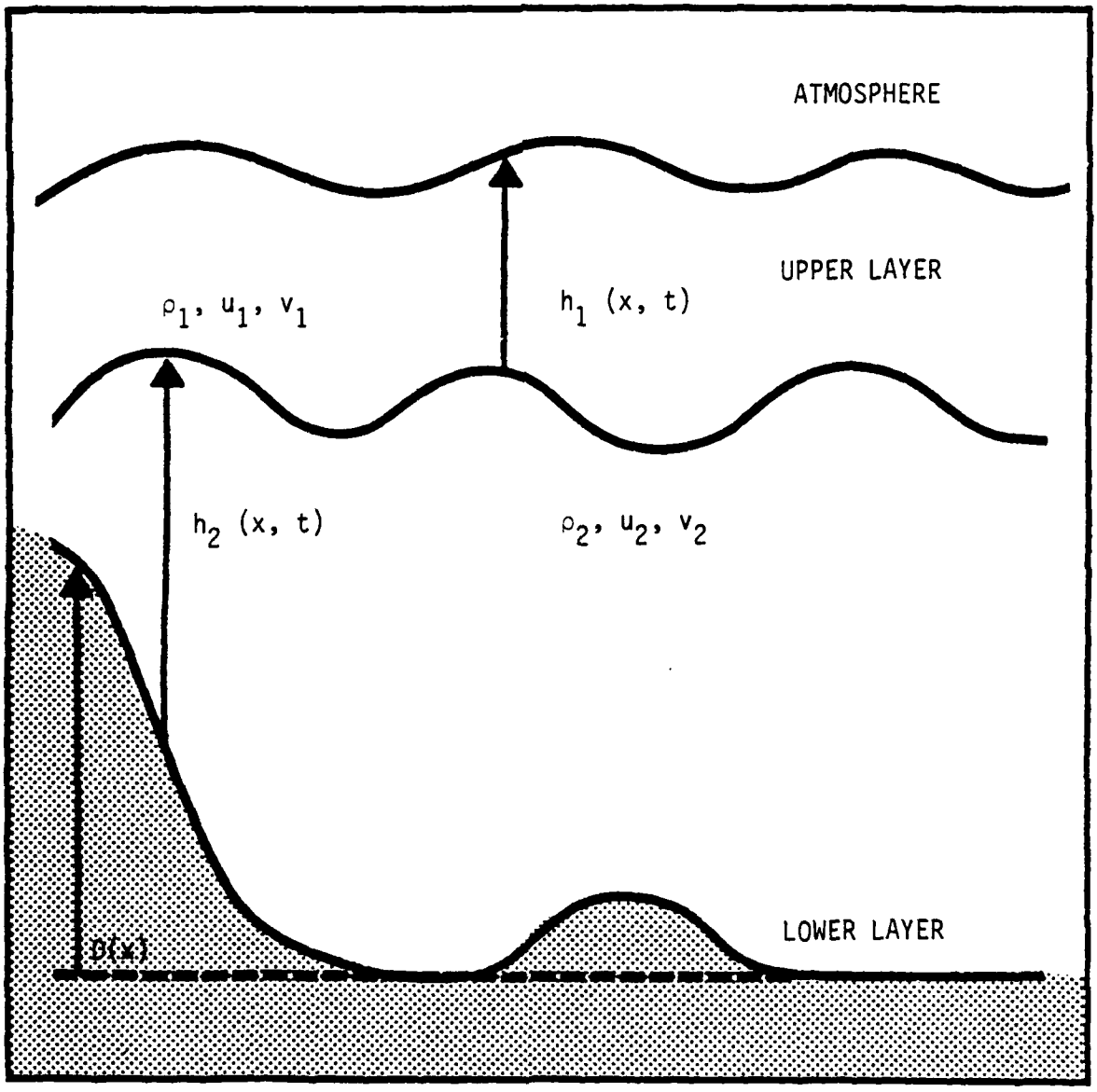

Figure 8. Two layer model cross section.

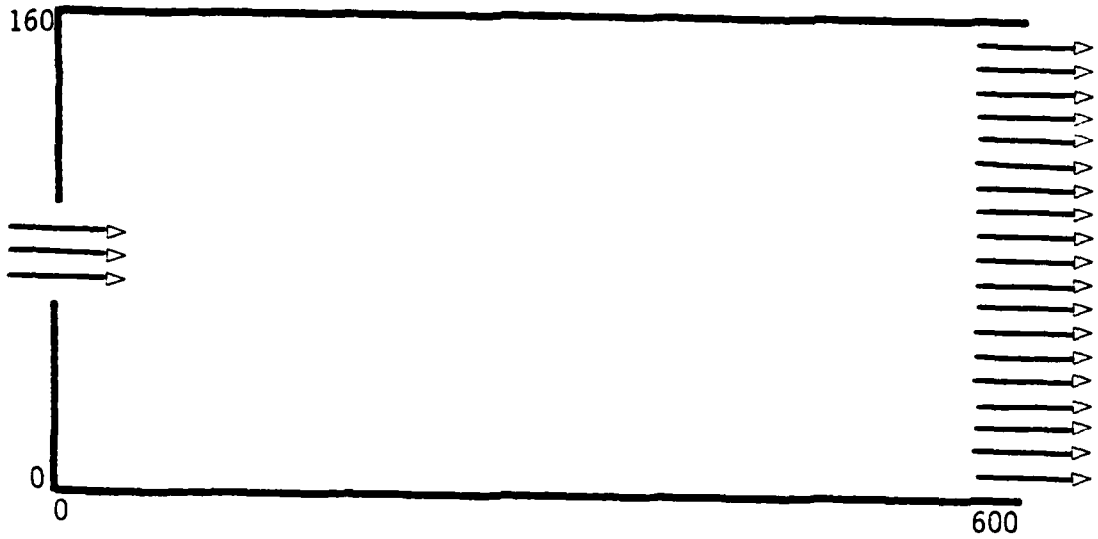

Figure 9a. Upper Layer

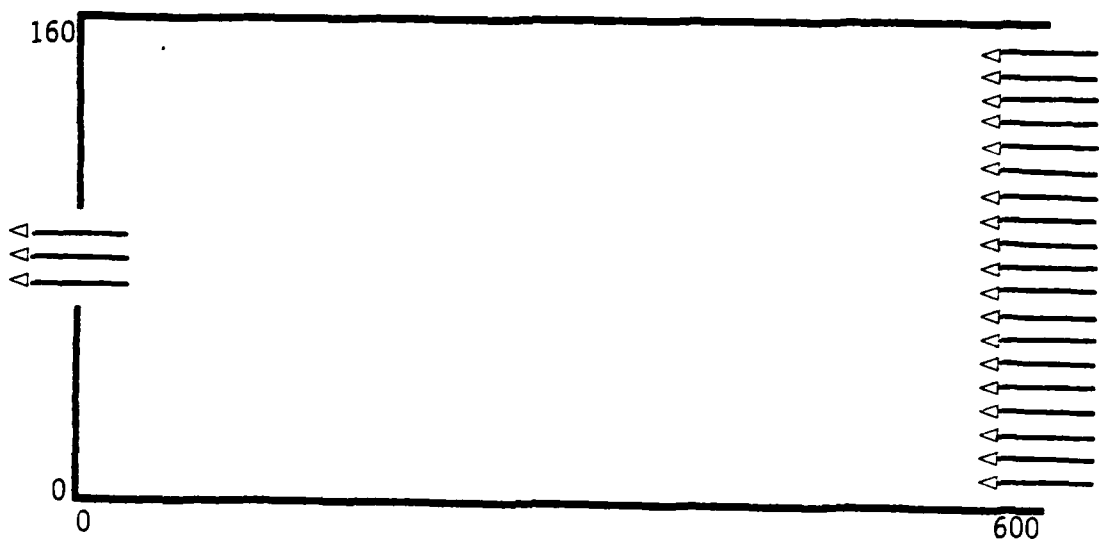

Figure 9b. Lower Layer

where

$$P_2 = P_1 - g'(h_1 - H_1)$$

In this first two layer experiment the model dimensions and configuration are identical to that of the reduced gravity model except that a uniform 2400 m deep lower layer has been added. Forcing in the upper layer remains the same as in the reduced gravity pivotal case except for the port location which has been moved to the exact center of the basin. The deep lower layer is forced with a westward moving flow from the open eastern boundary. This flow is kept at a uniform .2 cm/sec across the boundary, a value which agrees with observations that near the Straits, lower layer flow is as high as 10 cm/sec. Outflow is allowed only through the narrow western port (Figure 9).

Figures 10a and 10b show a comparison after 300 days of model integration of the reduced gravity (Figure 10a) and two layer (Figure 10b) cases. Note there is very little difference in the location, size and shape of the gyre in the two cases. Thus, the simple one layer model seems to represent all of the important features of the two layer flat bottom case.

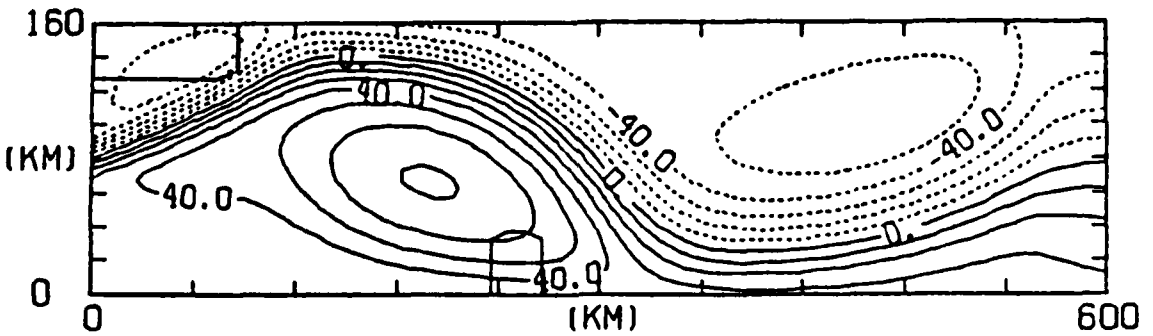

Figure 10a. Reduced gravity model solution.

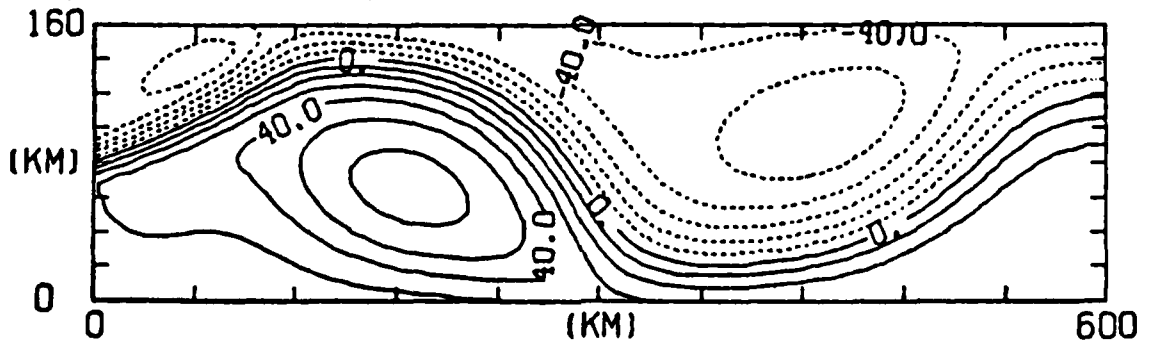

Figure 10b. Two layer model solution.

4. SUMMARY AND FUTURE WORK

The nonlinear, semi-implicit, reduced gravity and two layer numerical model (Hurlburt and Thompson, 1980) have been adapted to study the circulation in the Alboran Sea. Model results using an idealized rectangular geometry (600 km x 160 km), no topography and a northeastward inflow through the Strait of Gibraltar show an anitcyclonic gyre similar in size, shape and location to the Alboran Gyre (Figure 2). These results closely resemble the dynamic height contours of Lanoix (Figure 1) and suggest that topography and particular coastline features are not necessary to create a gyre with realistic dimensions and location. However, model results for the eastern Alboran show a series of cyclonic and anticyclonic circulations of much larger scale and smaller variability than observed. Additional numerical experiments showed the importance of the inflow angle and inflow vorticity in determining the size and location of the Alboran Gyre. When an additional uniformly flat lower layer with weak westward flow is included, little difference is observed between the reduced gravity and two layer solutions.

This paper has presented preliminary results of an attempt to model the Alboran Sea. Future work will include an investigation of the model dynamics, more realistic models, in particular two layer models including geometry and topography, and interaction with a field experiment.

REFERENCES

Bethoux, J. P., 1979. Budgets of the Mediterranean Sea. Their dependence on the local climate and on characteristics of the Atlantic waters. Oceanol. Acta. 2, 2: 137-163.

Burkov, V.A., Drivosheya, V.G., Ovchinnikov, I. M. and Savin, M. T., 1979. Eddies in the current system of the western Mediterranean Basin. Oceanology, 19: 9-13.

Cheney, R. E., 1977. Recent observations of the Alboran Sea front. NAVOCEANO Technical Note 370073-77, 24 pp.

Cheney, R. E., 1978. Recent observations of the Alboran Sea frontal system. J. Geophys. Res,. 83: 4593-4597.

Gallagher, J. J., Fecher, M. and Gorman, J., 1981. Project HUELVA oceanographic/acoustic investigation of the western Alboran Sea. NUSC Technical Report 6023, 106 pp.

Gascard, J. C., 1982. Mechanism of deep water formation in the North-Western Mediterranean. In: J. C. J. Nichoul (Editor), Hydrodynamics of semi-enclosed seas. Elsevier, Amsterdam, pp.

Groussson, R. and Faroux, J. 1963. Measure de courants de surface en Mer d'Alboran. Cah. Oceanogr., 15: 716-721.

Haltiner, G. J. and Martin, F. L., 1957. Dynamical and Physical Meteorology. McGraw-Hill, pp. 470.

Hurlburt, H. E. and Thompson, J. D., 1980. A numerical study of Loop Current intrusions and eddy shedding. J. Phys. Oceanogr., 10: 1611-1651.

Katz, E. J., 1972. The Levantine intermediate water between the Strait of Sicily and the Strait of Gibraltar. Deep Sea Res., 19: 507-520.

Lacombe, H., 1961. Contribution A L'Etude du Regime du Detroit de Gibraltar. Cah. Oceanogr., XIII: 74-107.

Lacombe, H. 1971. Le Detroit de Gibraltar. Note et Memoires de Service Geologique du Maroc., No 222 bis, 111-146.

Lacombe, H., 1982. Regime of the Strait of Gibraltar and of its east and west approaches. In: J. C. J. Nihoul (Editor), Hydrodymanics of semi-enclosed seas. Elsevier, Amsterdam, pp.

Lanoix, F., 1974. Project Alboran Etude Hydrologique Dynamique de la Mer d'Alboran. Tech. report 66, N. Atl. Treaty Org. Bussels, pp 39.

Mommsen, D. B., Jr., 1978. The effect of wind on sea surface temperature gradients in the Strait of Gibraltar and Alboran Sea. Report from Fleet Weather Central, Rota, Spain, 18 pp.

Nof, D., 1978. On geostrophic adjustment in Sea straits and estuaries: theory and laboratory experiments. Part II: Two-layer system. J. Phys. Oceanogr., 8: 861-872.

Ovchinnikov, I. M., 1966. Circulation in the surface and intermediate layers of the Mediterranean. Oceanology, 6: 48-59.

Ovchinnikov, I .M. , Krivosheya, V. G. and Maskalenko, L. V., 1976. Anomalous features of the water circulation of the Alboran Sea during the summer of 1962. Oceanology, 15: 31-35.

Peluchon, G. and Donguy, J. R., 1962. Travaux Oceanographiques d "l'Origny" dans le Detroit de Gibraltar. Compaigne internationale - 15 mpi, 15 Juin 1961. Zemi partie. Hydrologie en Mer d'Alboran. Cah. Oceanogr., 14: 573-578.

Petit, M., Klaus, V. Gelci, R., Fusey, F., Thery, J. J. and Bouly, P., 1978. Etude d'un tourbillon oceanique d'echelle moyenne en mer d'Alboran par emploi conjoint techniques spatiales et oceangraphiques. C. R. Acad. Sci. 287: 215-218.

Porter, D. L., 1976. The anticyclonic gyre of the Alboran Sea, Independent research report from M.I.T.-WHOI joint program, Woods Hole, Ma, pp 29.

Stevenson, R. W., 1977. Huelva Front and Malaga, Spain eddy chains as defined by satellite and oceanographic data. Deut. Hydrogr. A. 30, 2: 51-53.

Stommel, H., Bryder, H. and Magelsdorf, P., 1973. Does some of the Mediterranean outflow come from great depth? Pure and Appl Geophysics. 105: 879-889.

Wannamaker, B., 1979. The Alboran Sea Gyre: Ship satellite and historical data SACLANT ASW Research Centre Reprot SR-30, La Spezia, Italy, 27 pp.

Whitehead, J. A. and Miller, A. R., 1979. Laboratory simulation of the gyre in the Alboran Sea. J. Geophys. Res. 84: 3733-3742.